

Generation of droplets with adjustable chemical concentrations based on fixed potential induced-charge electro-osmosis

Yupan Wu^{*abc}, Bowen Hu^a, Xun Ma^a, Haohao Zhang^a, Wei Li^a, Yucheng Wang^a, and Shaoxi Wang^{*a}

^aSchool of Microelectronics, Northwestern Polytechnical University, Xi'an, PR China 710072, Email: wyp721@nwpu.edu.cn and shxwang@nwpu.edu.cn

^bResearch & Development Institute of Northwestern Polytechnical University in Shenzhen, PR China 518000

^cYangtze River Delta Research Institute of NPU, Taicang, PR China 215400.

Theoretical background

Electric field

The electrical potential in the bulk electrolyte can be calculated by solving Laplace's equation, assuming the bulk concentration is homogeneous.

$$\nabla \cdot (\sigma \mathbf{E}) = -\sigma \nabla^2 \phi = 0, \quad (\text{S1})$$

where \mathbf{E} is the electric field, ϕ is the bulk potential, and σ is the liquid conductivity.

The Laplace equation is subjected to the boundary conditions as follows:

At the driving electrodes, the boundary conditions are shown as follows:

$$\text{One: } \phi(t) = V_1 \cos(\omega t), \text{ and the other ground: } \phi(t) = 0. \quad (\text{S2a})$$

At the insulating surface, the boundary condition can be simplified to

$$\frac{\partial \phi}{\partial y} = 0 \quad (\text{S2b})$$

The double layer on the electrode describes the charging of the induced double layer owing to the current in the bulk. In the case of low voltage across the diffuse layer, the surface conservation equation is:

$$C_D \frac{d\zeta}{dt} = C_0 \frac{d\psi_0}{dt} = \frac{d(\phi_g - \phi)}{dt} \frac{C_D}{1 + \delta} = -\sigma \hat{n} \cdot \nabla \phi = \sigma \mathbf{E}_n, \quad (\text{S2c})$$

where $\zeta = V_g \cos(\omega t + \theta_g) - \phi(t)$ is the zeta potential, θ_g is the phase gap in the applied gate potential with reference to the driving signal. V_1 and V_g are the voltage amplitude applied to the driving electrode and BPE electrode, respectively. $V_g = V_{g1}$ for the left BPE and $V_g = V_{g2}$ for the right BPE

(Figure 1a). $\phi(t)$ is the potential in the bulk just outside the double layer. $C_0 = \frac{C_s C_D}{C_s + C_D} = \frac{C_D}{1 + \delta}$ is the capacitance per unit of area of the whole induced double layer, the parameter $\delta = C_D / C_s$ is the ratio of the diffuse layer capacitance ($C_D = \varepsilon / \lambda_D$) to Stern layer capacitance (C_s), ε is the permittivity, $\lambda_D = \sqrt{D\varepsilon / \sigma}$ is the Debye screening length, $D = 2 \times 10^{-9} \text{ m}^2/\text{s}$ is the bulk diffusivity and $\varepsilon = 7.08 \times 10^{-10} \text{ F/m}$ is the permittivity.

As for fixed-potential ICEO, an analytical solution for the induced zeta potential in the DC limit can be achieved as follows,

(1) When the BPE is floating, the induced zeta potential is

$$\zeta(t) = \frac{1}{1+\delta} \left(\frac{V_1}{2} \cos(\omega t) - \phi(t) \right) = \frac{1}{1+\delta} E x \cos(\omega t) \quad (S3)$$

The ICEO slip velocity on the surface of the floating electrode is given by the Helmholtz-Smoluchowski equation:

$$\langle \mathbf{v}_s \rangle = \frac{-\varepsilon}{\eta} \left\langle \frac{1}{1+\delta} E x \cos(\omega t) \cdot \mathbf{E}_t \right\rangle = \frac{-\varepsilon E^2 x}{2\eta(1+\delta)} \quad (S4)$$

(2) Assuming the phase gap $\theta_g = 0$, when an electric signal $V_g \cos(\omega t)$ is applied to the BPE, the zeta potential becomes:

$$\zeta(t) = \frac{1}{1+\delta} (V_g \cos(\omega t) - \phi(t)) = \frac{1}{1+\delta} \left(E x \cos(\omega t) + \left(V_g - \frac{V_1}{2} \right) \cos(\omega t) \right) \quad (S5)$$

The ICEO slip expression becomes:

$$\langle \mathbf{v}_s \rangle = \frac{-\varepsilon}{\eta} \left\langle \frac{1}{1+\delta} \left(E x \cos(\omega t) + \left(V_g - \frac{V_1}{2} \right) \cos(\omega t) \right) \cdot \mathbf{E}_t \right\rangle = \frac{-\varepsilon E}{2\eta(1+\delta)} \left(E x + V_g - \frac{V_1}{2} \right) \quad (S6)$$

The flow stagnation line (FSL) can be achieved by making $\langle \mathbf{v}_s \rangle$ equal to zero, it can be seen that, the FSL is located at the center of the floating electrode ($x=0$) when the gate electrode is set as

floating. Whereas, the FSL can be changed $\left(x = \frac{1}{E} \left(\frac{V_1}{2} - V_g \right) \right)$ by altering the electric signal $V_g \cos(\omega t)$. For instance, when the BPE is energized with $V_g \cos(\omega t)$ ($V_g > V_1/2$), positive charges will be accumulated at the top surface of the BPE, resulting in the formation of a negatively charged double layer in the liquid above the gate electrode. Consequently, an asymmetric ICEO flow occurs and FSL is directed away from the ground electrode. On the other hand, when $V_g < V_1/2$, a positively charged double layer forms and FSL is directed toward the ground electrode. Eq. (5) and (6) show that altering the electric potential applied to the gate electrode will change the zeta potential above the gate electrode, resulting in shifting the flow stagnation line and generating asymmetric flow across the channel. The direction of the asymmetry can also be reversed by changing the potential of the gate electrode. With the ability to actively fix the potential of the BPE, the asymmetric ICEO vortex can be used to generate effective mixing.

According to equation(4), an ICEO flow driven by the electric field occurs as long as the double layer has time to form when the applied frequency is low enough ($\omega < 1/\tau_c$). $\tau_c = \frac{\varepsilon L}{\sigma \lambda_D} = \frac{\lambda_D L}{D}$ is the "RC time" of an equivalent circuit of double-layer capacitors and bulk resistors of size L (here, L is the length scale).

When the metal strip is subjected to an external electric field initially, the electric field lines intersect normal to the surface, driving negative ions in solution toward one half of the surface ($x>0$) and positive ions to the other half, resulting in forming a dipolar induce double layer.

After a characteristic double layer charging time τ_c , the steady state can be achieved, in which the double layer totally insulates the surface and the field lines outside the double layer become tangential to the surface, leading to an ICEO flow.

From above we can see, the potential of the floating electrode is coupled to the external circuit and it acts like a driving electrode, thus fixed potential ICEO is closed related to ACEO. Meanwhile, it shows the same fundamental physical mechanism of ICEO, as the primary ICEO flow can occur in polarizable surface.

Flow field

For a Newtonian incompressible flow, the liquid motion can be obtained by solving the Navier-Stokes equations and the continuity equation in the limit of a small Reynolds number.

$$\rho \left(\frac{\partial \bar{\mathbf{v}}}{\partial t} \right) = \eta \nabla^2 \bar{\mathbf{v}} - \nabla p, \quad \nabla \cdot \bar{\mathbf{v}} = 0, \quad (S7)$$

P is the pressure, $\bar{\mathbf{v}}$ is the velocity.

For thin double layers and weak fields, the time-averaged slip velocity at the interface between the bulk and the double layer can be derived from the Helmholtz-Smoluchowski formula¹.

$$\langle \mathbf{v}_s \rangle = \frac{-\varepsilon}{\eta} \frac{1}{2} \text{Re} \left(\zeta \tilde{\mathbf{E}}_t^* \right) = \frac{-\varepsilon}{\eta} \frac{1}{1+\delta} \frac{1}{2} \text{Re} \left((\tilde{\phi}_s - \tilde{\phi}) (\tilde{\mathbf{E}} - \tilde{\mathbf{E}} \cdot \mathbf{n} \cdot \mathbf{n})^* \right), \quad (\text{S8a})$$

where \mathbf{E}_t is the tangential electric field, ζ is the zeta potential, η is the viscosity of the fluid, the asterisk indicates the complex conjugate. Although some equilibrium potential may exist on the channel walls, it can be safely neglected here due to linear electroosmotic slip, whose time-averaged value is zero in an AC field. Thus, the above equation can be set as the boundary condition on the surfaces of the electrodes.

$$\bar{\mathbf{v}} = \bar{\mathbf{v}}_0 \text{ at inlet and } P = 0 \text{ at outlet}, \quad (\text{S8b})$$

whereas, all other surfaces should be treated as no slip walls.

Concentration field

Assuming that electrophoretic effect is neglected, the mass transport equation can be written as

$$\frac{\partial C}{\partial t} + \bar{\mathbf{v}} \nabla C = D \nabla^2 C, \quad (\text{S9})$$

where C is the concentration of the species. The boundary conditions: the concentration values are set as 0 and 1 at the two inlets respectively, the channel walls and outlet are specified as $\mathbf{n} \cdot (-D \nabla C) = 0$.

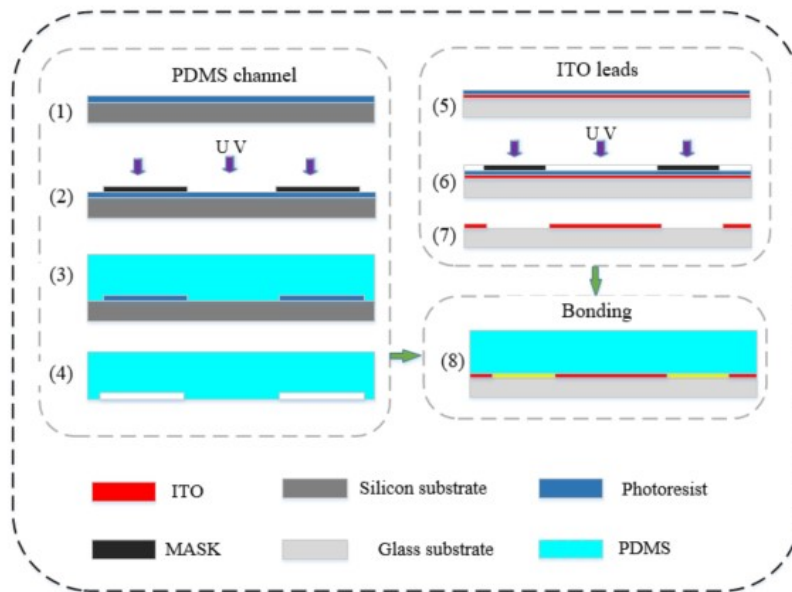


Figure S1) Schematic illustration of the fabrication process of the microfluidic device including: (1)-(4) fabrication of microchannel, (5)-(7) ITO electrode patterning, (8) plasma bonding.

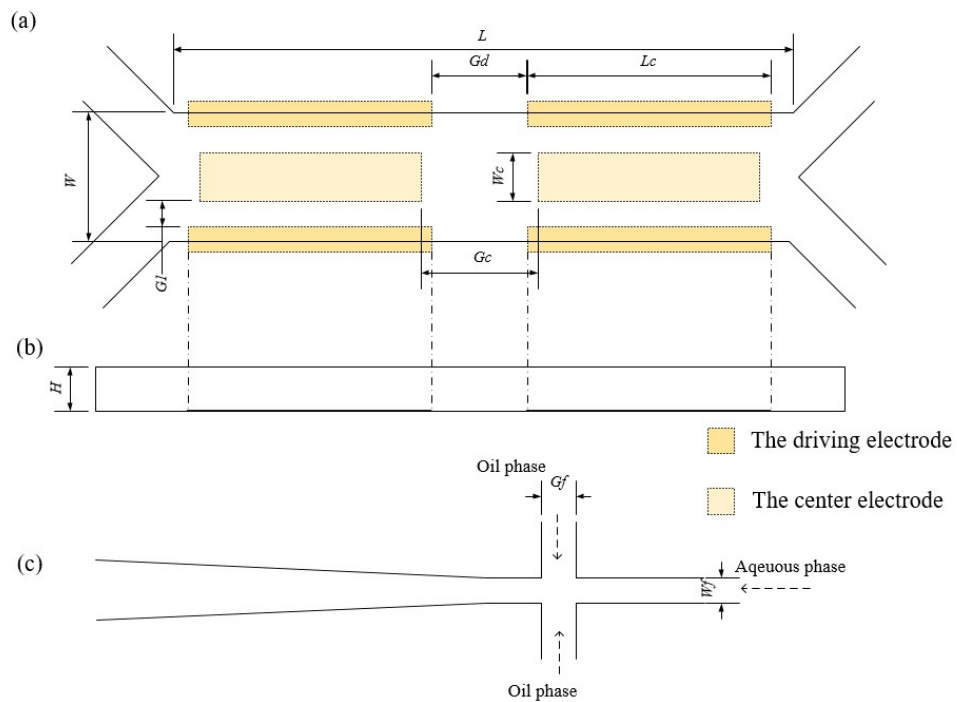


Figure S2 Schematic view of the integrated chip showing the mixing region (a and b) and droplet generation region (c).

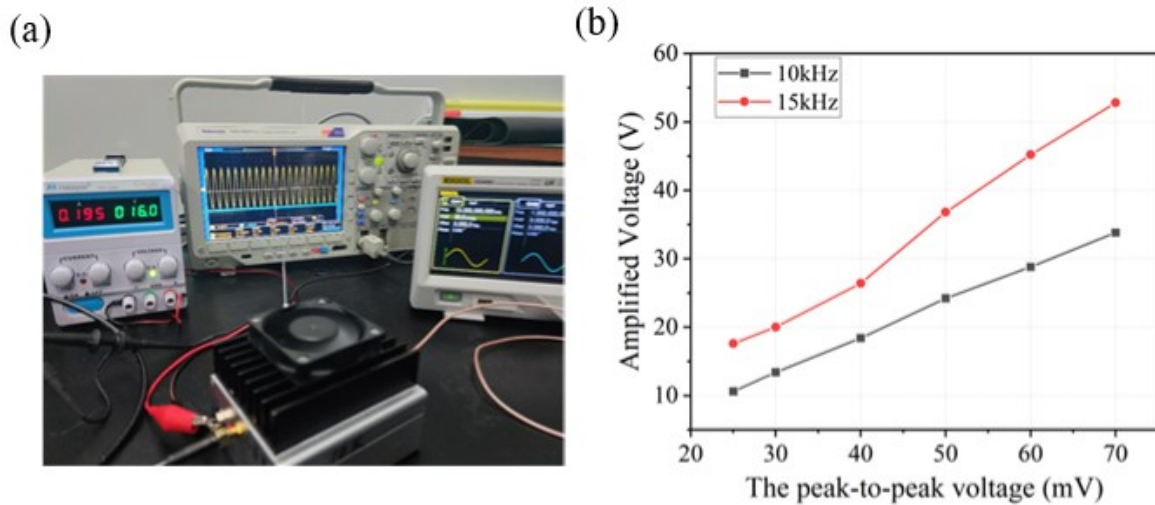


Figure S3 (a) Picture showing the process of generating an amplified signal using a power amplifier. (b) Amplified voltage displayed on oscilloscopes when applying different voltages ranging from 25mV to 70mV at 10kHz and 15kHz using the signal generator.

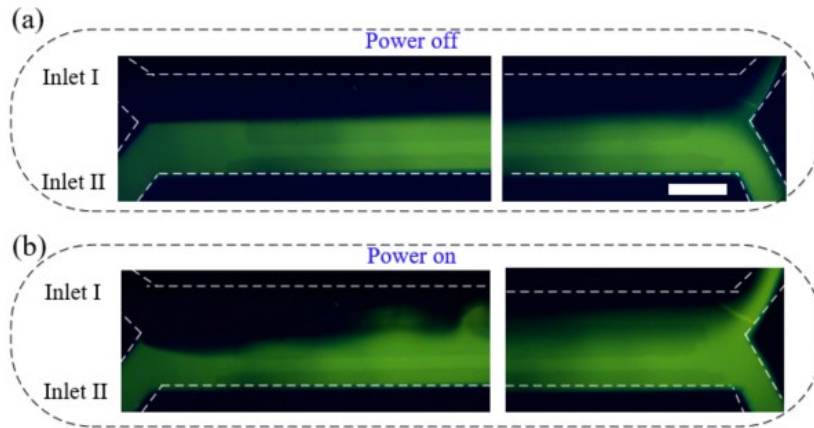


Figure S4. Fluorescence images of the sample in the mixing region without (a) and with (b) an electric field. Scale bar, 200 μm .

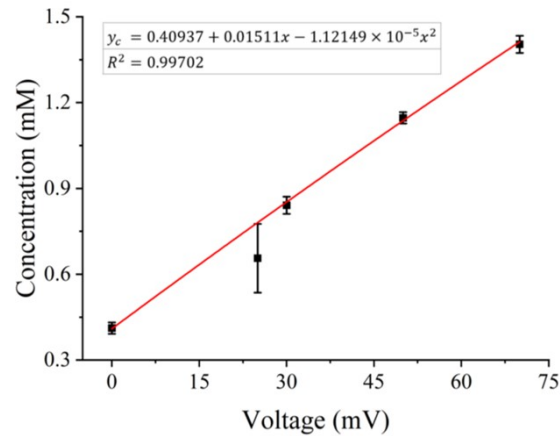


Figure S5 Calibration curve of in-droplet concentration as a function of the applied voltage

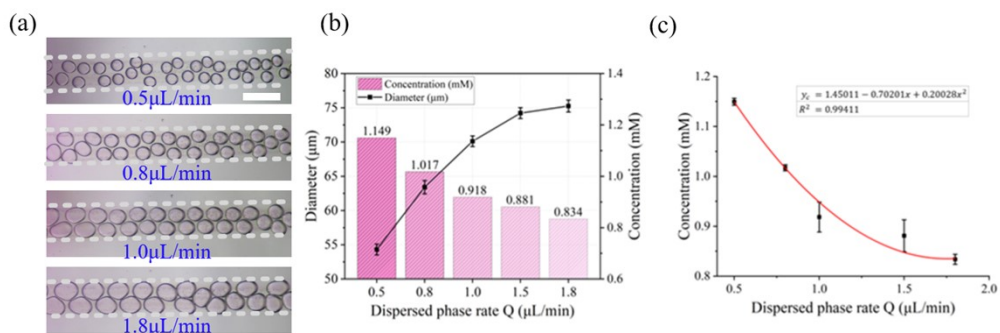


Figure S6 (a) Dependence of droplet diameter versus the flow rate of aqueous phase. (b) In-droplet concentration versus the aqueous phase rate at the constant flow rate of oil phase $Q_{oil} = 1.8 \mu\text{L}/\text{min}$ when $V_{g2} = V_1 = 50 \text{mV}$, $V_{g1} = \text{ground}$. Scale bar, $100 \mu\text{m}$. (c) Calibration curve of in-droplet concentration as a function of the flow rate of the aqueous phase.

Table S1. An overview of recently reported microdevice for generating droplets with tunable concentrations.

METHOD	DISADVANTAGE	ADVANTAGE	DROPLETS VOLUME	CONCENTRATION RANGE	APPLICATION	REF
Compartment on demand platform	Require a robotic sampler	Precise control over the droplets	Low nanoliter range	2-40mM	Enzyme kinetics and inhibition	²
Static droplet arrays	Low throughput (60 drops)	Modulating reagent concentration by 5 orders of magnitude.	30 nL	10 ⁻⁸ -10 ⁻³ M	Fluorescein, blue and yellow dye	³
Merging droplet with known concentrations	Require a piezoelectric actuator	Without microelectrode fabrication	1-10nL	2.4-4.2 (pH)	Malachite Green, and bromophenol blue indicator	⁴
Parallel flow-focusing methodology	Complicated and Multi-layered structure	Easy to implement	In nL-pL volumes	0-10 μM	Enzyme activity assay	⁵
Nanoliter-scale injection technique	Require an automated sample injection and driving systems	Wide concentration gradient	In nL-pL volumes	3-4 orders of magnitudes	enzyme inhibition assay of β-galactosidase	⁶
Microvalve-based method	Require pneumatic PDMS microvalves.	Flexible control of droplets	1.3-13.3nL	Not mentioned,	Four colored ink solution	⁷
Droplet dilutor	Require flow stabilization over a timescale	Simple and high-throughput	500pL-5nL	100μM-36nM	Fluorescein	⁸
Flow focusing/elect ric field	Need an AC field	Low cost, easy to use, dynamic and precise control	0.2-0.5nL	0.3-1.41mM	Fluorescein, and Rhodamine B	This work

(1) Bazant, M. Z.; Squires, T. M. Induced-charge electrokinetic phenomena: theory and microfluidic applications, *Phys Rev Lett* **2004**, *92*, 066101.

(2) Gielen, F.; van Vliet, L.; Koprowski, B. T.; Devenish, S. R.; Fischlechner, M.; Edel, J. B.; Niu, X.; deMello,

A. J.; Hollfelder, F. A fully unsupervised compartment-on-demand platform for precise nanoliter assays of time-dependent steady-state enzyme kinetics and inhibition, *Anal Chem* **2013**, *85*, 4761-4769.

(3) Sun, M.; Bithi, S. S.; Vanapalli, S. A. Microfluidic static droplet arrays with tuneable gradients in material composition, *Lab Chip* **2011**, *11*, 3949-3952.

(4) Shemesh, J.; Nir, A.; Bransky, A.; Levenberg, S. Coalescence-assisted generation of single nanoliter droplets with predefined composition, *Lab Chip* **2011**, *11*, 3225-3230.

(5) Damean, N.; Olguin, L. F.; Hollfelder, F.; Abell, C.; Huck, W. T. Simultaneous measurement of reactions in microdroplets filled by concentration gradients, *Lab Chip* **2009**, *9*, 1707-1713.

(6) Cai, L. F.; Zhu, Y.; Du, G. S.; Fang, Q. Droplet-based microfluidic flow injection system with large-scale concentration gradient by a single nanoliter-scale injection for enzyme inhibition assay, *Anal Chem* **2012**, *84*, 446-452.

(7) Zeng, S.; Li, B.; Su, X.; Qin, J.; Lin, B. Microvalve-actuated precise control of individual droplets in microfluidic devices, *Lab Chip* **2009**, *9*, 1340-1343.

(8) Niu, X.; Gielen, F.; Edel, J. B.; deMello, A. J. A microdroplet dilutor for high-throughput screening, *Nat Chem* **2011**, *3*, 437-442.